Supported lipid bilayers, tethered lipid vesicles, and vesicle fusion investigated using gravimetric, plasmonic, and microscopy techniques

Fredrik Höök[a)]
Division of Solid State Physics, Lund University, SE-22100 Lund, Sweden
and Department of Applied Physics, Chalmers University of Technology, Göteborg SE-41296, Sweden

Gudrun Stengel
Division of Solid State Physics, Lund University, SE-22100 Lund, Sweden

Andreas B. Dahlin
Division of Solid State Physics, Lund University, SE-22100 Lund, Sweden
and Department of Applied Physics, Chalmers University of Technology, Göteborg SE-41296, Sweden

Anders Gunnarsson, Magnus P. Jonsson, and Peter Jönsson
Division of Solid State Physics, Lund University, SE-22100 Lund, Sweden

Erik Reimhult[b)]
Department of Applied Physics, Chalmers University of Technology, Göteborg SE-41296, Sweden

Lisa Simonsson
Division of Solid State Physics, Lund University, SE-22100 Lund, Sweden

Sofia Svedhem
Department of Applied Physics, Chalmers University of Technology, Göteborg SE-41296, Sweden

(Received 24 January 2008; accepted 23 May 2008; published 31 July 2008)

This article summarizes our most recent contributions to the rapidly growing field of supported lipid assemblies with emphasis on current studies addressing both fundamental and applied aspects of supported lipid bilayer (SLB) and tethered lipid vesicles (TLVs) to be utilized in sensing applications. The new insights obtained from combining the quartz crystal microbalance with dissipation monitoring technique with surface plasmon resonance are described, and we also present recent studies in which nanoplasmonic sensing has been used in studies of SLBs and TLVs. To gain full control over the spatial arrangement of TLVs in both two and three dimensions, we have developed a method for site-selective and sequence-specific sorting of DNA-tagged vesicles to surfaces modified with complementary DNA. The combination of this method with nanoplasmonic sensing formats is covered as well as the possibility of using DNA-modified vesicles for the detection of unlabeled DNA targets on the single-molecule level. Finally, a new method for membrane fusion induced by hybridization of vesicle-anchored DNA is demonstrated, including new results on content mixing obtained with vesicle populations encapsulating short, complementary DNA strands. © *2008 American Vacuum Society.* [DOI: 10.1116/1.2948313]

I. INTRODUCTION

Artificial mimics of the natural cell membrane formed on solid supports have emerged as popular model systems in various branches of fundamental research, where the focus is on the essential role of the cell membrane for the integrity and function of cells in all living organisms. Since the cell membrane and its components also constitute common targets in disease diagnosis and for therapeutic drugs, the integration of cell-membrane mimics with surface-based bioanalytical sensors is expected to play an increasingly important role in future drug screening and diagnostic assays. Depending on the questions addressed and the techniques used, the requirements on the properties of the supported cell membrane mimics vary significantly. One of the most popular strategies is to form planar SLBs via lipid-vesicle adsorption and spontaneous rupture on silica-based materials or mica. First reported by McConnel *et al.*,[1] this method provides continuous laterally fluid planar SLBs, to be formed over macroscopic areas, thus being compatible with a large arsenal of analytical tools. The method was also proven compatible with formation of membrane-protein containing SLBs, [2] but concerns were raised regarding the influence from the close contact between the lipid membrane and the solid support on the function of the protein and its lateral mobility. To overcome this problem, and to simultaneously provide sufficient space underneath the membrane for studies of the membrane-protein controlled molecular trasnport, various ways to anchor planer lipid membranes via chemical tethers have been developed. [3–5] The planar configuration of SLBs and tethered lipid bilayers (TLBs) is also particularly important when highly oriented samples are required, for example,

[a)]Author to whom correspondence should be addressed; Tel.: +46-31-7726109; electronic mail: fredrik.hook@chalmers.se
[b)]Present address: Swiss Federal Institute of Technology Zurich (ETH Zürich), CH-8093 Zurich, Switzerland.

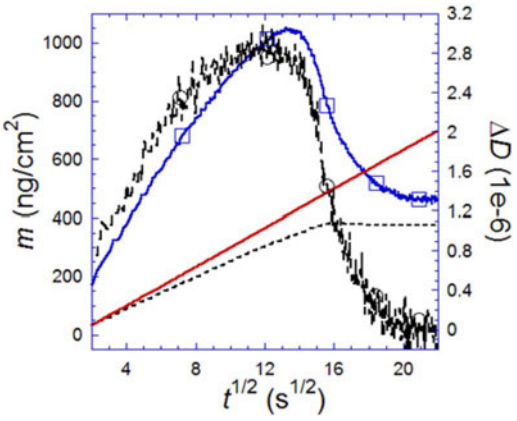

FIG. 1. Simultaneously measured QCM-*D* mass (solid blue line, squares) and damping (ΔD, dashed black line, circles) and SPR mass (dashed black line) responses as a function of $t^{1/2}$ for adsorption of ~55 nm mean diameter vesicles on SiO_2. QCM measured mass is calculated with Voigt-Kelvin modeling and the SPR measured mass through Fresnel and Lorenz-Lorentz modeling. For comparison the expected mass uptake from mass-transport limited adsorption is included (solid line), illustrating that (i) the adsorption is close to mass-transport limited for the major part of the adsorption and (ii) the mass-conversion of the SPR response is accurate. The figure is reproduced from Ref. 20.

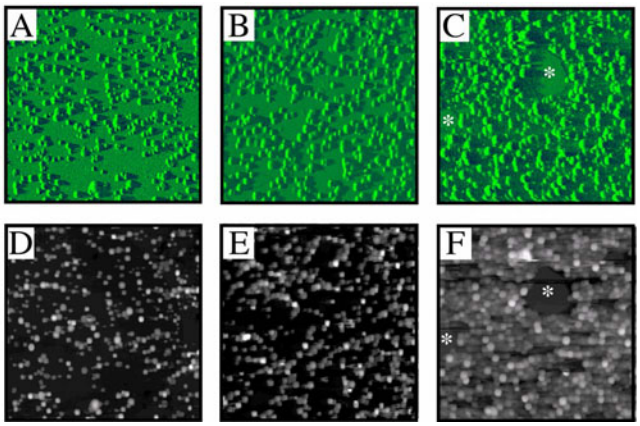

FIG. 2. AFM deflection images with corresponding composite height images in panels A-C and D-F, respectively, where D-F are images filtered by a subtraction procedure using both the trace and retrace height images (see Ref. 9 for details). The images are representative snapshots of a silica substrate, which was exposed to a vesicle solution for 45, 75, and 140 s, respectively, before it was rinsed with and subsequently imaged in pure buffer. The image size for all images is 4×4 μm; the height scales are 91.5, 95.0, and 91.5 nm for D, E and F, respectively. As exposure time is increased, vesicles (circular protrusions) become more and more abundant and for the longest exposure time, bilayer patches (asterisk) are observed. The figure is reproduced from Ref. 21.

in studies of two dimensional protein crystals,[6] lipid domain formation,[7] and lateral diffusivity of anchored biomolecular assemblies.[8]

However, in many cases, the aim of using supported lipid assemblies is to combine them with surface-based sensors to study kinetics of biorecognition reactions. In this case, a monolayer of TLVs is an attractive alternative. The most popular strategy involves lipid vesicles attachment through biotin-streptavidin binding,[9] but also alternative strategies involving hydrophobic anchors[10] and DNA tethers[11,12] exist. Although the volume enclosed by a single TLV is on the attoliter scale, they have been shown to be applicable also in studies of molecular transport reactions,[13] summarized in a recent review.[14]

In this paper, we summarize the contribution from our group to the fundamental and applied aspects of SLB formation and the use of SLBs and TLVs in various sensing applications, with particular focus on quartz crystal microbalance with dissipation (QCMD) monitoring and sensing based on both localized and conventional surface plasmon resonance (SPR).

II. SUPPORTED LIPID BILAYERS

A. Combined QCM-*D* and surface plasmon resonance studies of supported lipid bilayers

In the mid-1990s, we contributed to the advancement of the QCM technique by introducing a technique of simultaneously recording changes in resonance frequency, f, and damping, D, with high time resolution by probing the oscillation decay of the crystal after excitation at the resonance frequency.[15] At that time, the QCM technique was already well established for studies of biomolecular recognition reactions[16] and had been applied in studies of SLBs.[17] The added value of combined f and D measurements for such studies and, in particular, of spontaneous SLB formation from adsorption of unilamellar vesicles on silica, stem from the contrasts in Δf and ΔD induced by adsorbed vesicles and planar SLBs.[18,19] Figure 1 displays the temporal variations in mass uptake (see figure legend) and damping, ΔD, after exposing a silicon dioxide coated QCM crystal to lipid vesicles at $t=0$ under conditions similar to those used by others.[1,2] Also shown in this figure are the associated changes in optical mass obtained from a synchronized measurement using SPR on a silica-coated SPR chip in a symmetrical flow cell.[20,21]

While the mass uptake obtained from QCM and SPR at completed bilayer formation ($t>7$ min) are fairly similar, the initial mass uptake differs significantly. Furthermore, during the initial stages of the process the temporal variation of ΔD seems to share certain characteristics with the temporal variation of the QCM measured mass, suggesting that the overestimation of the mass uptake from QCM at low coverage is strongly correlated with the high damping. Taking into account that the damping induced by the complete SLB is virtually zero, the obvious interpretation of the initial increase in damping is that it reflects adsorption of unruptured vesicles. This picture was confirmed by atomic force microscopy (AFM) imaging of the SLB formation process when the adsorption process was interrupted by rinsing at selected times, as shown in Fig. 2. The AFM images illustrate accumulation of vesicles on the surface up to the point in time at which the damping reaches plateau ($t\sim140$ s).

It is important to note that the higher mass observed with QCM-*D* compared to SPR is not due to the damping introduced by the viscoelastic load on the crystal since this has been taken into account by modeling the data using a Voigt-

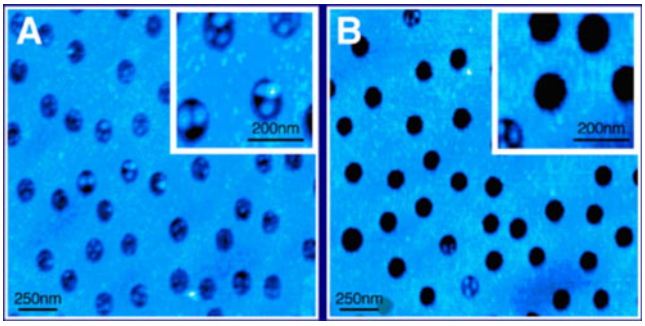

FIG. 3. AFM topography scans of a nanohole structure after exposure to biotin-bovine serum albumin (BSA) (which binds on Au but not on SiO_2) and vesicles ($\varnothing \sim 40$ nm, which binds preferentially to SiO_2 over biotin-BSA modified Au), in (A) the absence and (B) presence of Ca^{2+} (10 mM $CaCl_2$). As detailed in Ref. 19, force vs distance curves verified the formation of SLB patches in a majority of the holes (appears black in B) when Ca^{2+} was present. The figure is reproduced from Ref. 31.

Kelvin viscoelastic element model to represent the adsorbed film. In fact, this kind of analysis reveals that direct translation of changes in frequency into mass using the traditional linear (Sauerbrey) relation, leads to an *underestimation* rather than an overestimation of the mass coupled to the oscillation.[22] Hence, one needs to consider the different transducer principles of the two sensor configurations to interpret the origin of this discrepancy correctly.

In brief, the QCM-*D* technique is based on the variation in the electromechanical response of a shear-oscillating piezoelectric quartz disk caused by, for example, biomolecule binding or structural transitions in the adsorbed films. As a consequence, the mass obtained from QCM-*D* measurements corresponds to the total mass coupled to the motion of the sensor crystal, including both the mass of the biomolecules and the solvent bound to or hydrodynamically coupled to the molecular film. In contrast, the measured SPR signal originates from altered conditions for resonant surface plasmon excitation due to changes in the interfacial refractive index. For a simple dielectric material there exists, to a first approximation, a nearly linear relation between the change in refractive index caused by biomolecule adsorption and the number of molecules at the interface. Using suitable calibration schemes, this information is sufficient to estimate the adsorbed mass of biomolecules.[23] Hence, the difference between the mass uptake obtained using QCM and SPR equals the amount of bound or dynamically coupled water sensed by the QCM. In combination with the information obtained from changes in *D* regarding the temporal variation in film rigidity (or variation in shear viscosity and shear modulus as obtained from the Voigt-Kelvin modeling of the QCM-*D* response), this provides entirely new insights into the structural changes of adsorbed films. Combined with the merit of the QCM technique to be compatible with essentially any material, as long as it can be deposited as a sufficiently thin (1–10 μm) film, have played a major role in our work of combining various miniaturized sensor concepts with studies of SLBs and TLVs.

B. Nanoplasmonic sensing for studies of SLBs

Classical affinity-based label-free sensors, such as SPR and QCM, have found numerous applications within the broad field of biointerface science and biotechnology, but it is not clear which of these techniques that will be major players in the rapidly developing field of label-free high throughput sensors for applications in proteomics, diagnostics, drug discovery, forensic detection, etc. It is clear, however, that the main emphasis is currently placed on sensor concepts that provide either significantly improved sensitivity, or reduced size of the sensing spots or, preferably, a combination of both. Recent promising examples include the use of semiconductor nanowires for DNA and protein detection,[24] oscillating high-*Q* cantilevers,[25] and high-*Q* optical microcavities.[26] Using the latter technique label-free detection of single proteins was recently realized for the first time by Armani *et al.*[26] A promising alternative is a variant of conventional SPR named localized SPR (LSPR).[27] LSPR is a resonant phenomenon that arises when light interacts with nanoscale structures in metals, and utilizing this phenomenon has become more and more popular as the transducer principle in bioanalytical sensor applications. The two primary merits of the latter technique are (i) that miniaturization down to the single particle format can be achieved,[28,29] which in principle makes the concept suitable for arrays of extremely high probe density and (ii) the fact that the readout is based on colorimetric changes of the sensing template,[30] which makes it directly compatible with low-cost microscopy read out. However, for several reasons, LSPR sensing devices are not directly compatible with measurements of lipid-membrane associated reactions. First, SLBs are preferably formed on other materials than metals, such as silica, and this preference complicates functionalization of LSPR sensors with SLBs. In addition, the often extremely high confinement of the electromagnetic fields (~ 10 nm from the metal surface) associated with nanoparticle localized surface plasmons makes LSPR unsuitable for work with TLVs since a bound vesicle (with a typical diameter of 50–200 nm) would, to a large extent, be situated outside the LSPR field.

One way of resolving the first point is to use nanometer size apertures in a thin Au film to create the LSPR sensor element. We have shown that by adopting this configuration on top of a silica-coated substrate, we could functionalize the silica bottom of the LSPR active apertures with SLB patches formed by self assembly, as illustrated in Fig. 3.[31]

An important finding of the latter study was the high degree of localization of the nanoplasmonic field to the void of the apertures. By directing protein binding to either both the gold and the SLB coated silica regions or to the gold region only, it was demonstrated that for randomly distributed but short range ordered holes (~ 13 holes/μm^2) with a diameter and depth of ~ 110 and ~ 20 nm, respectively, at least 50% of the measured response was due to protein binding on SLB patches formed at the bottom of the holes.

To make the LSPR concept compatible with sensing of extended and laterally fluid bilayers formed via vesicle adsorption and spontaneous rupture (see above), a similar

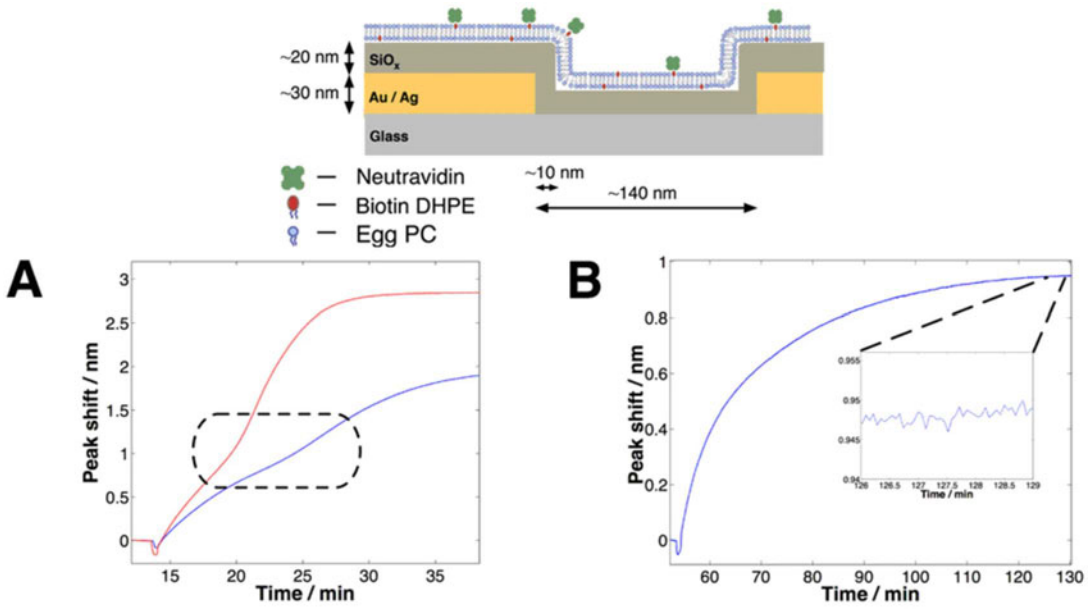

FIG. 4. Schematic illustration of the LSPR sensing template (top). (a) LSPR peak shift versus time upon exposure of the silicon oxide encapsulated Au (red) and Ag (blue) nanohole samples to suspended lipid vesicles ($t \sim 13$ min). The black dashed line marks the signature for SLB formation (see main text). (b) Same type of data as in (a) upon exposure of a biotin-containing SLB (5 wt %) to Neutravidin. Peak position shifts were probed as described in Ref. 30, providing a noise level of less then 10^{-3} nm and a data acquisition rate of ~ 1 s. The figure is reproduced from Ref. 32.

nanohole structure (diameter and depth of 140 and 30 nm, respectively) was fully encapsulated in a thin layer (approximately 20 nm) of silicon oxide. Besides providing the desired surface chemistry for spontaneous bilayer formation from vesicle adsorption, confirmed by fluorescence recovery after photobleaching demonstrating formation of laterally fluid bilayers, the silicon oxide layer also protects the underlying metal from, for example, oxidation. This enabled a fair comparison between identically shaped nanostructures in gold and silver (easily oxidized), of which the latter has been indicated in the literature to provide high sensitivity.[28] The difference in sensitivity between Au and Ag is demonstrated in Fig. 4(A), where the temporal variation of the shift in LSPR resonance wavelength is probed during SLB formation.[32]

Interestingly, at least for this particular type of nanostructure, gold was proven around 50% more sensitive than silver to biomolecular adsorption. Furthermore, for both metals, the sensitivity was reduced by the silicon oxide layer but was still surprisingly high. This indicates a longer decay length than usually reported for nanoplasmonic active particles[33] but is in agreement with recent work by Rindzevicius *et al.*[34] on apertures formed in thin metal films. This interesting observation is currently a subject of theoretical analysis.

Also note in Fig. 4(A) that the initial monotonic increase in the peak shift ($15 \text{ min} < t < 20$ min), which is attributed to adsorption of unruptured vesicles (see above), is followed by a slow but significant acceleration resulting in a kink-shaped curve. Interestingly, we know from the QCM-*D* data (see Fig. 1) that adsorbed vesicles rupture at a given coverage, suggesting that the characteristic shape of the response is attributed to SLB formation. To interpret this observation,

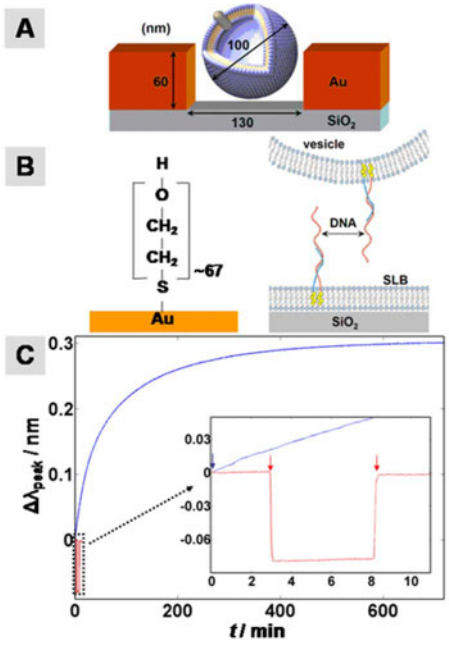

FIG. 5. [(A) and (B)] Schematics of vesicle attachment inside a nanohole: thiol-PEG makes Au inert to vesicle binding while lipid bilayer patches can be formed on the bottom of the nanoholes. Lipophilic (cholesterol-modified) DNA strands were used to link vesicles to the bilayer inside the holes through sequence-specific hybridization. (C) Peak shift vs time upon addition of DNA-modified vesicles to a PEG and DNA-modified functionalized nanohole template. The response upon addition of vesicles modified with noncomplementary DNA, added at $t=3$ min followed by rinsing at $t=8$ min, is shown in red. Response from vesicles modified with complementary DNA (introduced at $t=0$) is shown in blue. The figure is reproduced from Ref. 35.

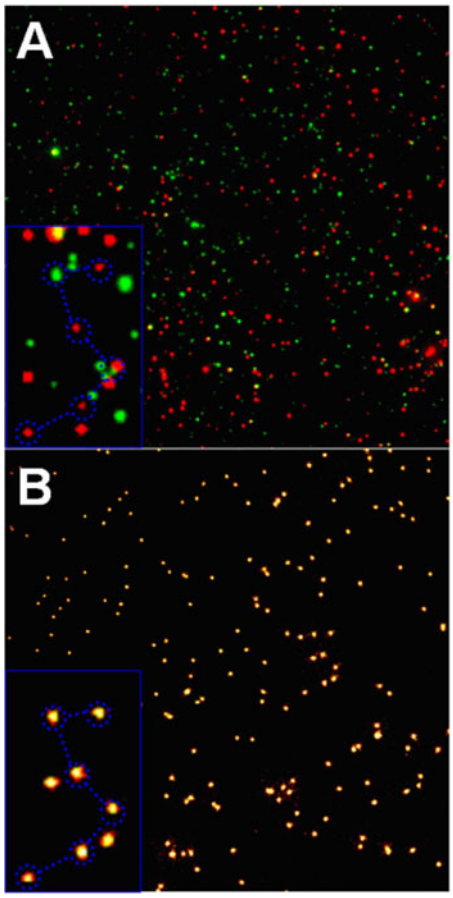

FIG. 6. TIR micrographs displaying (a) red and green vesicles bound on a particular location (field of view 100×100 μm^2) on a nanohole sample. Yellow spots represent green and red vesicles in close proximity on the sample (not separated beyond the spatial resolution). Micrograph (b) shows the nanoholes at the same location, imaged as elastic scattering objects. The insets show magnifications of a particular location and illustrate a typical correlation of the positions of nanoholes and vesicles. The figure is reproduced from Ref. 35.

one must recall that the intensity of the evanescent field, and the sensitivity of the LSPR response, is highest at, and decays away from, the sensor surface. During the vesicle-rupture process, lipids associated with adsorbed vesicles move closer to the surface and thereby into a region where the LSPR field strength is higher. As a consequence, during the vesicle-rupture process, the magnitude of the peak shift (at a given time interval) is expected to have a positive contribution from not only adsorption of vesicles, but also vesicles that rupture. Hence, the observed acceleration in the LSPR response is attributed not to acceleration in the actual mass deposition, but to a structural change of the already adsorbed vesicles. To the best of our knowledge, this is the first example illustrating the use of the shallow evanescent field of LSPR active templates to probe biomacromolecular structural changes without the introduction of external labels. We also emphasize the potential of the template for studies of cell membrane linked biorecognition reactions, as illustrated by the detection of Neutravidin to a fraction of biotin-modified lipids in the SLB with a signal-to-noise ratio of around 500 [Fig. 4(B)], which is good even in comparison with state of the art label-free sensors.

III. TETHERED LIPID VESICLES

A. Nanoplasmonic sensing for studies of TLVs

One potentially attractive use of LSPR active apertures is for studies of material transport into and/or out of tethered lipid vesicles. With a somewhat deeper sensing depth than that associated with discrete nanoparticles and with the plasmonic field strongly confined to the void of the apertures, successful positioning of single vesicles into individual apertures is expected to localize a significant fraction of the field to the interior of the vesicles. With such an arrangement, transport of material through the vesicle membrane accompanied by a change in local refractive index within the vesicle would allow a direct measure of material transport through a cell membrane mimic. The high speed by which the colorimetric changes in LSPR templates can be probed (<10 ms),[30] and the relatively large signals that are expected from such material transport, makes this principle very attractive for functional studies of the different classes of membrane-residing proteins responsible for cell membrane transport, including ion channels, aquaporines, fusion proteins, peptide, protein translocators, etc. As a first step toward this goal, we extended our work on material-specific surface modifications of plasmonic apertures in gold (see Fig. 3) by introducing a long poly(ethylene glycol)-based (~70 EG units) surface modification of gold that made it highly inert to vesicle adsorption. After formation of nanoscale SLB patches on silicon oxide in the bottom of the holes (see above) water-soluble lipophilic DNA (see further below) was self-inserted into the SLB patches. Subsequently, lipid vesicles modified with complementary lipophilic DNA were added. As shown in Fig. 5, DNA-guided vesicle binding was selective with a clearly detectable peak position shift, and, as shown in Fig. 6, the localization of single vesicles to the nanoscale apertures could be confirmed (see inset) by combined total internal reflection (TIR) dark-field imaging and fluorescence microscopy.[35] It appears from this image that most vesicles appear to bind outside the holes. This is simply because samples with far fewer nanoholes were used in the microscopy measurements. See Ref. 35 for details.

Based on the measured sensitivity to changes in bulk refractive index (~220 nm/RI unit) and the absolute peak position shifts upon bilayer patch formation and vesicle binding of ~0.17 and ~0.3 nm, respectively, it could be estimated that only about 1% of the sensing capacity was "used up" by the lipid shell of the TLVs. Under the very reasonable assumptions that (i) the decay depth increases with increasing depth of the apertures (which was 55 nm in this case) and (ii) that the plasmonic field is strongest in the void of the holes, this suggests that the template holds significant promise for studying *transport* across lipid membranes since a significant fraction of the probing volume remains unoccupied and is expected to be available for detecting changes in index of

refraction *within* the tethered vesicles. Realization of such transport studies using optical rather than, for example, electrical signal transduction will require integration with fluidics that provides sufficiently rapid liquid exchange or mixing at the site of detection. Such development is currently undertaken in our group.

B. Site-selective sorting of TLVs

Our work on DNA-modified lipid vesicles was inspired by Niemeyer and co-workers who in the mid-1990s introduced the concept of modifying water-soluble proteins modified with short single-stranded DNA for site-specific and sequence-selective protein sorting on arrays composed of complementary DNA.[36,37] The merit of this approach is essentially twofold. First, by modifying a library of proteins with different DNA sequences, a protein array can be formed spontaneously as soon as a DNA array is exposed to a mixture of DNA-tagged proteins. Second, while short DNA strands are robust molecules which sustain drying even when immobilized, proteins are more fragile and prone to losing their structural integrity and hence function upon both immobilization and drying. The most conventional methods for fabricating protein arrays involve dispensing of the protein solutions, followed by a drying step. Our initial motivation for the development of DNA-modified vesicles illustrated in the previous section was to transfer the DNA-hybridization based sorting principle from water-soluble proteins to lipid vesicles carrying membrane-residing proteins. While, in parallel efforts, Yoshina-Ishii and Boxer used chemically activated lipid head groups to couple short single-stranded DNA to lipid vesicles for similar purposes,[12] we used self-inserting lipophilic cholesterol-modified DNA,[38] initially developed to enhance the cellular uptake of antisense DNA by lipidation.[39] Cholesterol-DNA was found to self-incorporate into the vesicle membrane, which apparently facilitated the preparation of DNA-tagged vesicles. However, membrane attachment by self-incorporation of cholesterol-modified DNA suffered from a severe drawback. Upon mixing of differently DNA-modified vesicles, the reversible nature of the membrane attachment resulted in rapid exchange of DNA between different vesicles. Vesicle sorting from a mixture of vesicles was thus not possible since the time required for exchange of cholesterol-DNA between vesicles was comparable to, or faster than, the time required for DNA-hybridization mediated binding to the surface. This, in turn, restricted our initial method to the sequential formation of arrays of vesicles. However, self-incorporation of amphiphilic DNA is in many cases advantageous, for instance when cell membranes extracted from living cells are used or when reactions between activated lipid head groups and membrane-residing compounds may lead to unwanted side reactions. Fortunately, the membrane affinity of DNA-modified cholesterol was shown to be significantly enhanced by anchoring DNA using two cholesterol moieties instead.[40] This was achieved by hybridizing a 15 bases long DNA strand modified with DNA in the 3′ end with a 30 bases long DNA strand modified with cholesterol in the 5′ end (see the schematic illustration in Fig. 5). This and similar DNA constructs have been and are currently used by us and others for site-selective sorting of vesicles in combination with optical wave guide lightmode spectroscopy (OWLS),[41] for studies of the lateral mobility of tethered vesicles[42,43] including the kinetics of DNA-hybridization induced docking events[44] and for studies of three-dimensional networks of lipid vesicles,[45] in which case the full sensing volume of conventional SPR sensors can be efficiently utilized.[46] As demonstrated in Sec. III C, DNA-modified vesicles can also be used as a convenient method for single-molecule detection of unlabeled DNA targets.

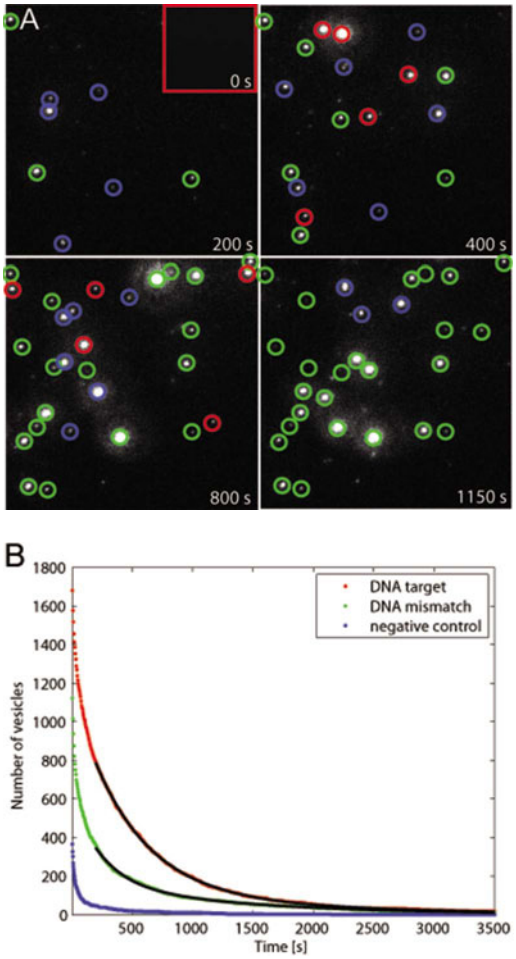

FIG. 7. (A) TIRF micrograph snapshots at various times after introduction of labeled vesicles to a DNA-modified surface pre-exposed to 30-mer DNA target strands (100 fM). Single vesicles are highlighted with color-coded rings to visualize the different processes. Green circles indicate vesicles that remain bound to the surface beyond the last frame of the measurement. Red circles highlight vesicles immobilized on the surface for at least ten frames, but that are released prior to the last fame of the measurement. Blue circles indicate vesicles only present for less than ten frames. Field of view is 90 $\times 90$ μm. (B) Curves showing, at a DNA concentration of 10 pM, the number of vesicles binding longer to the surface than a certain binding time, but that has lost contact with the surface before the last frame of the measurement. The black curves are curve fits to the DNA target and DNA mismatch data points for $t \geq 200$ s, which yields the dissociation constant describing the residence time behavior (Ref. 36). The restricted range for the curves fits are to avoid the influence of nontarget mediated binding as seen in the negative control curve. The figures are reproduced from Ref. 47.

C. Single-molecule detection utilizing TLVs

We recently demonstrated how the fact that single vesicles are easily detected using conventional fluorescence microscopy (see, for example, Fig. 5) can be exploited to probe unlabeled DNA strands.[47] Using TIR fluorescence (TIRF) microscopy, unlabeled 30 bases long DNA targets were detected at low femtomolar concentrations by using the DNA target to mediate the binding of DNA-modified vesicles to a DNA-modified surface. Under the condition that the average lateral separation of DNA on the surface was larger than the average vesicle diameter and by ensuring that the probability of having more than one DNA, anchored via two cholesterol moieties, per vesicle was low, essentially each vesicle that remained bound on the surface was controlled by a single DNA target. Furthermore, using TIRF as the mode of detection, it was ensured that only vesicles present within the evanescent field at the interfaces were detected [Fig. 7(A)]. By continuous time-lapse imaging, combined with suitable image analysis that selects for the vesicles that remain bound on the surface, not only single-molecule detection was proven feasible. In fact, by investigating the residence time of vesicles in the bound state, single-molecule reaction kinetics could be obtained. This is illustrated in Fig. 7(B), which displays the residence time of vesicles whose presence on the surface was mediated by fully complementary or single mismatch 30-mer DNA targets.

This method is, in particular, attractive since (i) ensemble reaction kinetics can be derived from statistics of multiple single-molecule binding and release events under equilibrium conditions, rather than from an analysis of the rate of binding and release upon rinsing, and since (ii) the single-molecule sensitivity provides kinetics to be extracted from low target concentrations (picomolar and even below). However, in deducing information from binding kinetics, it is important to be aware that a subpopulation of the immobilized vesicles will be affected by photobleaching. Distinguishing between vesicles that disappear from the surface due to bleaching in contrast to vesicles that lose contact due to DNA unbinding is made by monitoring the intensity profile of each vesicle as a function of time. A vesicle is marked as bleached if the intensity gradually drops below an intensity value, chosen slightly above the noise floor. In contrast, if the intensity drop is sudden and not gradual, the vesicle is considered to have lost contact with the surface. For the data in Fig. 7(B), the fraction of bleached vesicles constitutes only a small part of the total number of vesicles that disappear from the surface. Furthermore, only vesicles that lose contact with the surface are included in the dissociation analysis, thus minimizing the effect of bleaching. See Ref. 47 for further details.

The method is also fully compatible with any type of sandwich assay, such as classical immunoassays. Since labeling of vesicles is convenient (already a few percent of fluorescently labeled lipids makes the vesicles easily detectable) and since their brightness is not quickly diminished by bleaching due to the large number of fluorophores, there are

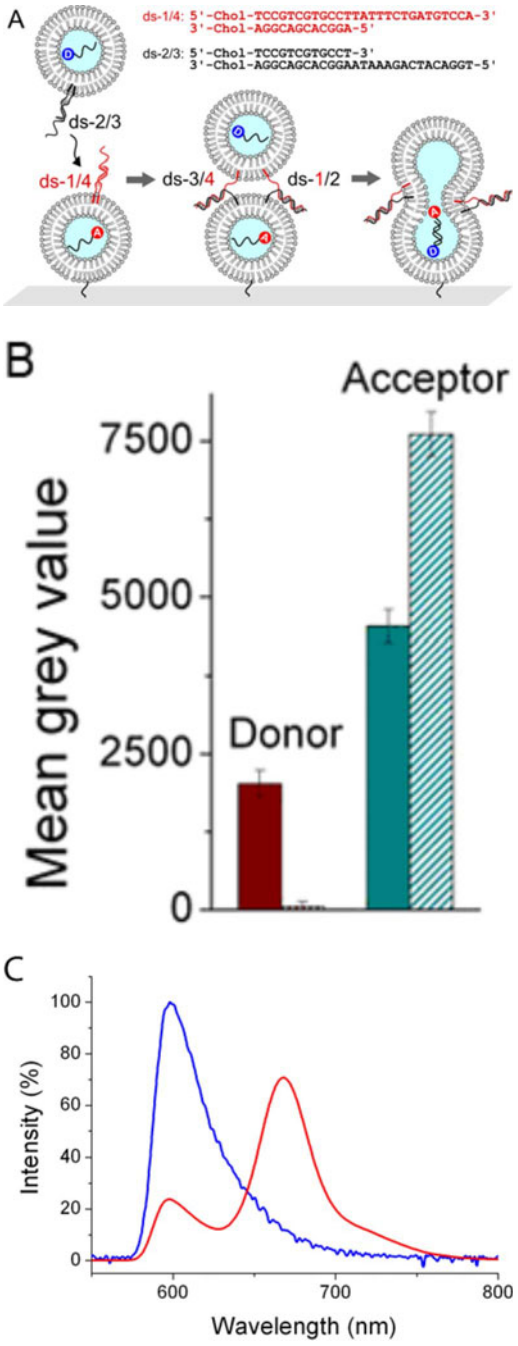

FIG. 8. Content mixing during DNA-mediated vesicle fusion demonstrated by transfer of encapsulated DNA. (A) Vesicles were modified with the double cholesterol-labeled DNA strands ds-1/4 and ds-2/3, respectively. As ds-1/4 and ds-2/3 encounter each other, they hybridize in a zipperlike fashion, thereby forming blunt-ended duplexes with 27 base pairs (ds-1/2) and 12 base pairs (ds-3/4) (middle) and opening a fusion pore. (B) The changes in donor (TAMRA, shown in brown) and acceptor (Cy5, shown in green) intensity observed for hybridization of encapsulated DNA during fusion. Solid bars present the intensity before and striped bars the intensity after addition of vesicles tagged with complementary fusion DNA. The encapsulated DNA used for the FRET-based content mixing assay were 5′-Cy5-AGTCCATGCGAC-3′ and 3′-TCAGGTACGCTG-TAMRA-5′. (C) Fluorescence emission spectrum from mixing TAMRA-DNA with an equal amount of Cy5–DNA free in solution ($\lambda_{excitation}$=555 nm). The curve in blue shows the emission spectrum of the donor DNA alone, whereas the curve in red shows the emission spectrum of the donor/acceptor-labeled DNA duplex, where the latter curve has been corrected for direct excitation of the acceptor.

good reasons to work with lipids rather than other optically labeled nanoparticles. However, the advantage of using lipid vesicles is especially large when it is difficult to fully passivate the particle surface while ensuring that only single probes are immobilized to the particle surface or in cases where membrane compounds are investigated. An example of the latter is biorecognition controlled membrane fusion (although this is not yet extended to studies on the single vesicle format in our group), a subject that is highlighted in Sec. III D

D. DNA-mediated programmable vesicle fusion

One particularly interesting process that involves close contact between two cell membranes is membrane fusion, which is generally catalyzed by specific fusion proteins that force two lipid membranes in sufficiently close contact for membrane fusion to occur.[48] Fusion proteins consist of a hydrophobic domain that inserts into the membrane and a water-soluble domain that protrudes from the membrane surface. The central function of the water-soluble domain is to bring two membranes into apposition whereas the transmembrane, hydrophobic segment is believed to cause lipid perturbations that facilitate fusion. We recently demonstrated how the biological fusion concept can be mimicked using membrane-anchored DNA strands.[49,50] In contrast to the DNA strands previously used to tether vesicles either to surfaces[12,40] or in three-dimensional networks,[46] the base sequence and directionality of fusion-inducing DNA was designed to bring about DNA hybridization in a zipperlike fashion [see Fig. 8(A)]. The change in hybridization geometry forces the membranes into closer proximity, which is an important determinant for spontaneous membrane fusion.

Using a lipid composition of DOPC/DOPE/CH (50/25/25) complete bilayer fusion could be verified in bulk, demonstrating both outer and inner leaflet mixing.[50] In a yet unpublished study, we designed a fluorescence resonance energy transfer (FRET)-based content mixing assay that was applied in the surface-based format: two different types of egg-PC vesicles ($\varnothing \sim 100$ nm) were prepared by extrusion, one encapsulating tetramethyl-6–carboxyrhodamine (TAMRA)-labeled 12-mer DNA (donor), the other one encapsulating Cy5-labeled complementary 12-mer DNA (acceptor). After coating glass microscope slides with a passivating layer of polylysine-grafted polyethylene glycol, two independent experiments were carried out where either donor-DNA or acceptor-DNA containing egg-PC vesicles were surface-tethered using biotin/streptavidin coupling. When donor-vesicles were immobilized first, fluorescence imaging was carried out using a standard TRITC filter cube with $\lambda_{excitation}=555$ nm/$\lambda_{emission}=580$ nm. When tethering the acceptor-dye containing vesicles first, we excited at $\lambda_{excitation}=555$ nm and collected the emission at $\lambda_{emission}=670$ nm. Thus, either the FRET-induced effects on the donor or on the acceptor emission were tracked. Upon immobilization, the vesicles retained their fluorescent content proving successful encapsulation of both donor and acceptor DNA. Microscope images were taken before and 1 h after addition of the acceptor-DNA (or donor-DNA) containing fusion vesicles, depending on which vesicle type was deposited in the first step. Free DNA was simply removed by thorough rinsing before acquisition of the images. Figure 8(B) displays a decrease in the donor channel intensity of nearly 100% after acceptor vesicles were added to the immobilized donor vesicles, and in the same way the acceptor channel intensity increased by 60% when donor vesicles were added to immobilized acceptor vesicles. To have a reference, we hybridized to a 1–to-1 ratio of TAMRA and Cy5–labeled DNA strands free in solution and recorded fluorescence emission spectra of the donor-DNA alone (blue) and of the donor/acceptor-labeled DNA duplex (red) (see Fig. 8(C)). In both experiments we observed anticorrelated changes in donor and acceptor intensity as characteristic for FRET. Thus, the encapsulated DNA strands hybridized as a consequence of content mixing due to membrane fusion in the surface experiments. Conversely, anticorrelated signal changes were not observed when we carried out the same experiment employing DNA that tethers vesicles carrying complementary DNA together but not in a zipperlike geometry (see above). Thus, only cholesterol-DNA zippers facilitated complete fusion of both bilayer leaflets. Although the efficiency of content mixing for different compounds, different lipid compositions and different DNA anchoring strategies remain to be investigated in future work, we anticipate that DNA-induced programmable membrane fusion will become a uniquely powerful tool for understanding the biophysics of membrane fusion in general and for targeted delivery of membrane-bound proteins and vesicle contents in particular.

IV. CONCLUDING REMARKS AND FUTURE OUTLOOKS

We emphasize that this overview of our most recent contribution to the field of supported lipid assemblies is a short summary highlighting the connections between some of the projects that are currently running in our group. Although several distinguished contributions by other groups working in the same and connected areas are not included we hope that we have inspired the readers to join and contribute to this exciting field of science. In our view, it appears clear that macroscopic sensors, such as QCM-*D* and SPR, but also ellipsometry, OWLS, impedance spectroscopy, etc., will continue to play key roles in this branch of research for decades to come. However, it also appears clear that nanoscale sensors have started to mature and will, as sufficiently powerful theories are developed, emerge as important analytical tools in both fundamental and applied branches that rely on supported lipid assemblies. Another interesting insight that becomes clearer and clearer relates to the question regarding which model system that will dominate the future applications involving supported lipid assemblies: supported planar lipid bilayers or tethered lipid vesicles? It seems as if the answer depends on the systems under investigation and the questions addressed. For label-free affinity sensing of, for example, ligand-receptor interactions, tethered vesicles ap-

pear the most attractive, since solutions have emerged that have the potential to handle the problems associated iwth both sorting and sensing on high density arrays. In cases when direct measurement of material transport across the membrane is in focus., tethered planar bilayers still appear the most attractive, but formation of high density arrays is a problem that remains to be solved in this case. However, with the evanescent field of, for example, plasmonic based sensors concentrated to the interior of tethered vesicles, material transport measurements based on changes in refractive index within the vesicles may be feasible. Another attractive component with plasmonically active apertures in thin metal films, is the fact that the substrate is conductive. Hence, plasmonic sensing could, in principle, be directly combined with electro chemistry and impedance spectroscopy in combination with both SLBs and TLVs. However, simultaneous label-free affinity sensing and direct measurement of membrane-protein mediated material transport still remains a vision, and it is far from clear which approach that will eventually enable such a combination. It is our strong belief, however, that the field of biointerface science has today reached a point where the understanding of self-assembly and self-organization of biological entities in general, and lipid assemblies in particular, and bottom-up and top-down nanoscale fabrication processes of transducer formats have matured to a stage where such a goal is no longer science fiction, but a highly realistic goal that can and will be realized in the not too distant future.

ACKNOWLEDGMENTS

The authors would like to thank the coauthors of some of the papers that are highlighted, in particular, Michael Zäch, who performed the AFM analysis, Jonas Tegenfeldt, who developed the TIRF setup, Indriati Pfeiffer, who introduced the double cholesterol anchor, and MSc. Raphael Zahn, who contributed to the membrane fusion project. The authors are also grateful to Bengt Kasemo, who stimulated the development of the QCM-*D* technique and its application to studies of SLBs. This work was financially supported by the Swedish Research Council, the Biomimetic, INGVAR and BIONANOIT programs funded by SSF and Vinnova and the Marie Curie Grant No. MEIF-CT-2006-039909.

[1]H. M. McConnell, T. H. Watts, R. M. Weis, and A. A. Brian, Biochim. Biophys. Acta **864**, 95 (1986).
[2]J. Salafsky, J. T. Groves, and S. G. Boxer, Biochemistry **35**, 14773 (1996).
[3]M. L. Wagner and L. K. Tamm, Biophys. J. **79**, 1400 (2000).
[4]R. Naumann, E. K. Schmidt, A. Jonczyk, K. Fendler, B. Kadenbach, T. Liebermann, A. Offenhausser, and W. Knoll, Biosens. Bioelectron. **14**, 651 (1999).
[5]T. Stora, J. H. Lakey, and H. Vogel, Angew. Chem., Int. Ed. **38**, 389 (1999).
[6]I. Reviakine, W. Bergsma-Schutter, and A. Brisson, J. Struct. Biol. **121**, 356 (1998).
[7]C. Dietrich, L. A. Bagatolli, Z. N. Volovyk, N. L. Thompson, M. Levi, K. Jacobson, and E. Gratton, Biophys. J. **80**, 1417 (2001).
[8]J. T. Groves, N. Ulman, and S. G. Boxer, Science **275**, 651 (1997).
[9]L. S. Jung, K. E. Nelson, P. S. Stayton, and C. T. Campbell, Langmuir **16**, 9421 (2000).
[10]M. A. Cooper, A. Hansson, S. Lofas, and D. H. Williams, Anal. Biochem. **277**, 196 (2000).
[11]S. Svedhem, D. Dahlborg, J. Ekeroth, J. Kelly, F. Hook, and J. Gold, Langmuir **19**, 6730 (2003).
[12]C. Yoshina-Ishii and S. G. Boxer, J. Am. Chem. Soc. **125**, 3696 (2003).
[13]D. Stamou, C. Duschl, E. Delamarche, and H. Vogel, Angew. Chem., Int. Ed. **42**, 5580 (2003).
[14]S. M. Christensen and D. Stamou, Soft Matter **3**, 828 (2007).
[15]M. Rodahl, F. Höök, A. Krozer, P. Brzezinski, and B. Kasemo, Rev. Sci. Instrum. **66**, 3924 (1995).
[16]M. Minunni, M. Mascini, G. G. Guilbault, and B. Hock, Anal. Lett. **28**, 749 (1995).
[17]P. A. Ohlsson, T. Tjarnhage, E. Herbai, S. Lofas, and G. Puu, Bioelectrochem. Bioenerg. **38**, 137 (1995).
[18]C. A. Keller, K. Glasmastar, V. P. Zhdanov, and B. Kasemo, Phys. Rev. Lett. **84**, 5443 (2000).
[19]C. A. Keller and B. Kasemo, Biophys. J. **75**, 1397 (1998).
[20]E. Reimhult, C. Larsson, B. Kasemo, and F. Hook, Anal. Chem. **76**, 7211 (2004).
[21]E. Reimhult, M. Zach, F. Hook, and B. Kasemo, Langmuir **22**, 3313 (2006).
[22]F. Hook, B. Kasemo, T. Nylander, C. Fant, K. Sott, and H. Elwing, Anal. Chem. **73**, 5796 (2001).
[23]L. S. Jung, C. T. Campbell, T. M. Chinowsky, M. N. Mar, and S. S. Yee, Langmuir **14**, 5636 (1998).
[24]F. Patolsky, G. F. Zheng, and C. M. Lieber, Anal. Chem. **78**, 4260 (2006).
[25]P. S. Waggoner and H. G. Craighead, Lab Chip **7**, 1238 (2007).
[26]A. M. Armani, R. P. Kulkarni, S. E. Fraser, R. C. Flagan, and K. J. Vahala, Science **317**, 783 (2007).
[27]K. A. Willets and R. P. Van Duyne, Annu. Rev. Phys. Chem. **58**, 267 (2007).
[28]A. D. McFarland and R. P. Van Duyne, Nano Lett. **3**, 1057 (2003).
[29]G. Raschke, S. Kowarik, T. Franzl, C. Sonnichsen, T. A. Klar, J. Feldmann, A. Nichtl, and K. Kurzinger, Nano Lett. **3**, 935 (2003).
[30]A. B. Dahlin, J. O. Tegenfeldt, and F. Hook, Anal. Chem. **78**, 4416 (2006).
[31]A. Dahlin, M. Zach, T. Rindzevicius, M. Kall, D. S. Sutherland, and F. Hook, J. Am. Chem. Soc. **127**, 5043 (2005).
[32]M. P. Jonsson, P. Jonsson, A. B. Dahlin, and F. Hook, Nano Lett. **7**, 3462 (2007).
[33]A. V. Whitney, J. W. Elam, S. L. Zou, A. V. Zinovev, P. C. Stair, G. C. Schatz, and R. P. Van Duyne, J. Phys. Chem. B **109**, 20522 (2005).
[34]T. Rindzevicius, Y. Alaverdyan, M. Kall, W. A. Murray, and W. L. Barnes, J. Phys. Chem. C **111**, 11806 (2007).
[35]A. Dahlin, M. Jonsson, and F. Hook, Adv. Mater. (Weinheim, Ger.) **20**, 1436 (2008).
[36]C. M. Niemeyer, Angew. Chem., Int. Ed. **40**, 4128 (2001).
[37]C. M. Niemeyer, T. Sano, C. L. Smith, and C. R. Cantor, Nucleic Acids Res. **22**, 5530 (1994).
[38]S. Svedhem, I. Pfeiffer, C. Larsson, C. Wingren, C. Borrebaeck, and F. Hook, ChemBioChem **4**, 339 (2003).
[39]R. G. Shea, J. C. Marsters, and N. Bischofberger, Nucleic Acids Res. **18**, 3777 (1990).
[40]I. Pfeiffer and F. Hook, J. Am. Chem. Soc. **126**, 10224 (2004).
[41]B. Stadler, D. Falconnet, I. Pfeiffer, F. Hook, and J. Voros, Langmuir **20**, 11348 (2004).
[42]J. J. Benkoski and F. Hook, J. Phys. Chem. B **109**, 9773 (2005).
[43]C. Yoshina-Ishii, Y. H. M. Chan, J. M. Johnson, L. A. Kung, P. Lenz, and S. G. Boxer, Langmuir **22**, 5682 (2006).
[44]Y. H. M. Chan, L. Peter, and S. G. Boxer, Proc. Natl. Acad. Sci. U.S.A. **104**, 19577 (2007).
[45]A. Graneli, M. Edvardsson, and F. Hook, ChemPhysChem **5**, 729 (2004).
[46]A. Granéli, J. J. Benkoski, and F. Hook, Anal. Biochem. **367**, 87 (2007).
[47]A. Gunnarsson, P. Jonsson, R. Marie, J. O. Tegenfeldt, and F. Hook, Nano Lett. **8**, 183 (2008).
[48]R. Jahn and H. Grubmuller, Curr. Opin. Cell Biol. **14**, 488 (2002).
[49]G. Stengel, L. Simonsson, R. A. Campbell, and F. Hook, J. Phys. Chem. B ASAP Article (2008).
[50]G. Stengel, R. Zahn, and F. Hook, J. Am. Chem. Soc. **129**, 9584 (2007).